Materials Letters 135 (2014) 67–70

Contents lists available at ScienceDirect

Materials Letters

journal homepage: www.elsevier.com/locate/matlet

# One-dimensional ordered growth of magneto-crystalline and biocompatible cobalt ferrite nano-needles

M. Ravichandran [a], Goldie Oza [b], S. Velumani [b,f,*], Jose Tapia Ramirez [c], Francisco Garcia-Sierra [d], Norma Barragán Andrade [d], Marco A. Garza-Navarro [e], Domingo I. Garcia-Gutierrez [e], R. Asomoza [b]

[a] Program on Nanoscience and Nanotechnology, CINVESTAV-IPN, Av IPN 6508, San Pedro Zacatenco, Mexico D.F, Mexico
[b] Department of Electrical Engineering, CINVESTAV-IPN, Av IPN 6508, San Pedro Zacatenco, Mexico D.F, Mexico
[c] Department of Genetics and Molecular Biology, CINVESTAV-IPN, Av IPN 6508, San Pedro Zacatenco, Mexico D.F, Mexico
[d] Department of Cell Biology, CINVESTAV-IPN, Av IPN 6508, San Pedro Zacatenco, Mexico D.F, Mexico
[e] Universidad Autónoma de Nuevo León, UANL, Nuevo León, Mexico
[f] School of Information and Communication Engineering, Sungkyunkwan University, 300 Cheoncheon-Dong, Jangan-Gu, Suwon, Republic of Korea

ARTICLE INFO

*Article history:*
Received 23 September 2013
Accepted 26 July 2014
Available online 4 August 2014

*Keywords:*
Cobalt ferrite
Co-precipitation
Nano-needles
Magnetization

ABSTRACT

In this letter, we have reported a novel synthesis of $CoFe_2O_4$ nano-needles by a co-precipitation method using precursors of ferric chloride and cobalt nitrate at 80 °C. The structural and magnetic properties of as-grown needle-like $CoFe_2O_4$ nanostructures exhibit cubic spinel structure. $CoFe_2O_4$ nano-needles have an average diameter of 15 nm with an aspect ratio of 30:50, which was depicted by High-resolution transmission electron microscopy (HRTEM). Superconducting Quantum Interference Device (SQUID) confirmed the property of superparamagnetism. The magnetic measurement illustrated that the coercivity (Hc) of $CoFe_2O_4$ nano-needles increased from −145.84 Oe at 5 K to −25.38 Oe at 312 K. The cell viability studies of $CoFe_2O_4$ nano-needles were performed in the concentration range of 5–1000 μg/ml on L6 (Skeletal muscle cell lines) and Hep-2 (Larynx carcinoma) cells using 3-(4,5 dimethylthiazol-2-yl)-2,5-diphenyltetrazolium bromide (MTT) assay. There was more than 50% cell viability for both the cell lines, but Hep-2 cells were more prone to killing as compared to L6 cells. Such biocompatible nanostructures can be used as drug-delivery systems for cancer therapeutics.



## 1. Introduction

Magnetic nanomaterials have intrigued the scientific community to enhance its mechanical hardness and biological activity. In the past decade, the synthesis of magnetic nanomaterials have been intensively studied due to the wide applications in biosensing, medical [1], and magnetic storage media [2]. The chemical routes for the synthesis of magnetic nanoparticles mainly include co-precipitation [3], microemulsions [4], sol–gel [5], and hydrothermal or solvothermal reactions [6]. The electrical, magnetic, thermal, chemical, and biomedical properties of nanomaterials strongly depend upon the structure and morphology of the particles. Hence, many efforts have been devoted to the manipulation of these factors to meet the needs for different applications. One-dimensional (1D) nanoscale materials have stimulated considerable interest recently because of their small dimension and thermodynamic stability [7]. Cobalt ferrite is a well-known hard magnetic material with high coercivity, moderate magnetization, high electromagnetic performance, excellent physical and chemical stability, mechanical hardness and high cubic magneto-crystalline anisotropy. There are many conventional techniques for preparation of cobalt ferrite but all of them have the disadvantage of agglomeration [8,9]. In this paper, we have presented one-pot synthesis of cobalt ferrite nano-needles by the co-precipitation method. The size and size distribution was regulated by controlling the nucleation and growth rates. When the nucleation rate was higher than the growth rate, smaller and uniformly distributed nano-needles were obtained during synthesis [10]. Cytotoxicity assay of such nanostructures were performed on L6 (Skeletal muscle cells) and Hep-2 (Larynx Carcinoma) using MTT for the comprehension of toxicity as well as their significance in the field of Nanomedicine.

## 2. Experimental section

The chemical reagents used for nano-needle synthesis were ferric chloride ($FeCl_3 \cdot 6H_2O$), Cobalt (II) nitrate Hexahydrate

* Corresponding author at: Department of Electrical Engineering (SEES), CINVESTAV-IPN, Av IPN 6508, San Pedro Zacatenco, Mexico D.F, Mexico.
*E-mail address:* velu@cinvestav.mx (S. Velumani).

http://dx.doi.org/10.1016/j.matlet.2014.07.154
0167-577X/

($CoN_2O_6 \cdot 6H_2O$), Sodium Hydroxide (NaOH) and Hydrochloric acid (HCl). All the chemicals were purchased from Sigma-Aldrich and were directly used without any further purification.

In a typical synthesis, 50 mL of degassed 1.5 M NaOH solution was used as a reducing agent under constant stirring. Then 10 mL of deionised water was degassed with nitrogen gas and then 0.0018 M of $CoN_2O_6 \bullet 6H_2O$, 0.0036 M of $FeCl_3 \bullet 6H_2O$, 0.85 mL of HCl were added. The solution mixture was then added to NaOH solution under constant stirring with nitrogen atmosphere at 80 °C for 1.5 h. The reaction is as follows:

$$2Fe^{3+} + Co^{2+} + 8OH^- \rightarrow CoFe_2O_4 + 4H_2O \quad (1)$$

Nitrogen gas was passed through the solution throughout the experiment to prevent the formation of hematite as well as to deaerate the system [12]. Later, black solid powders were separated by using a magnet. The particles were then washed with distilled water for three times. The final product was dried in a desiccator for 24hrs.

## 3. Results and discussions

X-ray diffraction (XRD) pattern (Fig. 1A) suggested the formation of cobalt ferrites with well-defined lattice planes of (111), (220), (311) and (400), which are signature markers of cobalt ferrite. The significance of nitrogen gas was proved by the absence of any hematite peak in XRD. The crystal size determined by Scherrer equation with XRD data is 14.8 nm, which is close to the particle size calculated from TEM images (14.6 nm). This indicates that $CoFe_2O_4$ is nanocrystalline in nature.

Transmission electron microscopic observation of black colored cobalt ferrites apparently showed formation of needle shaped morphologies (Fig. 2A). The aspect ratio of the needles is in the range of 30–50 with sharp tips. Furthermore, evidence of the nanostructure was given in Fig. 2B from HR-TEM micrographs and Inverse Fast Fourier Transform (IFFT) diffractogram (inset of Fig. 2B). They display well-crystallized cobalt ferrite nano-needles with a lattice fringe of 0.25 nm, which is very close to the interplanar spacing of (311) plane of the ferrite crystal phase.

Energy dispersive X-ray (EDX) spectrometer analysis confirmed the stoichiometric ratio of ~2:1 for Fe and Co (Fig. 2C). In addition, selected area electron diffraction (SAED) patterns in Fig. 2D show several discernible concentric rings, which revealed crystalline spinel phase structure of the needles.

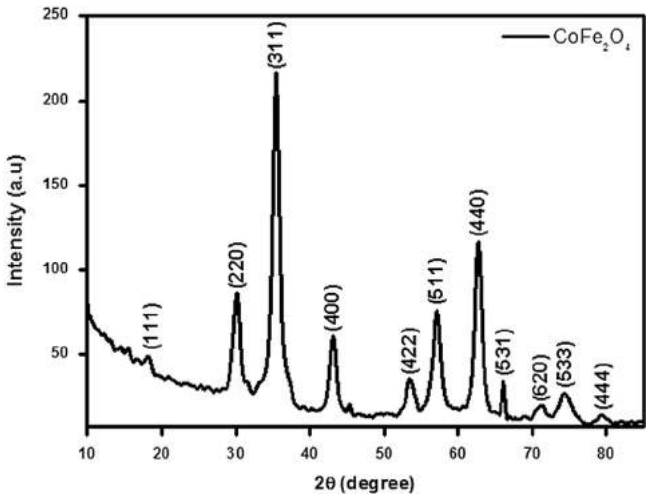


**Fig. 1.** XRD patterns of the $CoFe_2O_4$ nano-needles synthesized by the co-precipitation.

The UV–visible spectrum of $CoFe_2O_4$ nano-needles is shown in Fig. S1 (see in Supplementary information). Examination of the spectra shows that the solution has absorption in the entire range of UV–vis spectrum, and absorption increases gradually with decrease in wavelength.

The magnetic properties of pure $CoFe_2O_4$ nano-needles were evaluated by SQUID. Typical magnetization hysteresis loops are shown in Fig. 3A and saturation magnetization (Ms), magnetic remanence (Mr), Hc values at 5, 300 and 312 K are presented in Table 1. The Hysteresis curve at 5 K suggest an analogous behavior to what is shown by a classic ferromagnet, with Ms=74 emu/g, and Mr=7.53 emu/g. However, the ratio of Mr/Ms=0.1 is lower than the one reported for ferromagnets with cubic anisotropy (magnetocrystallinity) of Mr/Ms=0.8, and was lower than the one observed on systems of nanostructures with a uniaxial anisotropy, Mr/Ms=0.5. This feature suggests that there is magneto-crystalline anisotropy acting over the relaxation of the magnetic moment of the nanostructures. This could be co-related to the shape of the needle-like morphology of the nanostructures. This suggests that the response of material to the applied field is dominated by the interactions of the particles, which seems to be of demagnetizing nature. On the other hand, the curves obtained at 300 and 312 K show an absence of measurable hysteretical characteristics, which suggests that at these temperatures the system is still under the superparamagnetic regime. This fact is based on the observation that both curves superimpose on each other almost perfectly. Thus, it suggests that the response of magnetization is dominated by the interactions among particles, such as the ones related to core-surface exchange in particles and not to surface phenomenon [5].

In the case of ZFC (Zero Field Cooling) curve (Fig. 3B), it can be noticed that no maximum can be observed which is normally attributed to the blocking temperature. This temperature indicates the value above which the system starts to show superparamagnetic characteristics. Moreover, it can be noticed that the FC (Field Cooling) curve shows irreversibility with respect to the ZFC curve [11]. The behavior of both curves is congruent with the observations made with respect to the response of the sample's magnetization as a function of applied field. This explains us that when the size of the magnetic materials is smaller than the superparamagnetic critical dimension, just above the blocking temperature, the thermal fluctuation of the particles will surely circumvent the anisotropy. This will cause rotation of the moments among the different easy directions and superparamagnetism is shown. The demagnetizing interactions within particles might be responsible for dipolar coupling among magnetic moments that are close enough to form a multidomain-like magnetic ordering in nano-needles.

Room temperature Raman spectra of as-synthesized cobalt ferrite samples showed in Fig. S2 (see in Supplementary information) show broad peaks at 474, 564, 636 $cm^{-1}$ and a strong peak at 682 $cm^{-1}$ which clearly indicates cubic structure, thus depicting four Raman active modes [A1g(2)+A1g(1)+T2g(3)+T2g (2)]. Due to difference in ionic radii of Co and Fe ions in $CoFe_2O_4$, where Fe alone occupies the tetrahedral site as well as Co and Fe occupies octahedral site, the Fe–O, Co–O bond distance redistribute between both the sites resulting in doublet like structure.

The biological property of these nanostructures for the application in the field of drug-delivery was analyzed using various concentrations of cobalt ferrite nano-needles ranging from 5–1000 μg/ml and then MTT assay was performed. Fig. 4 demonstrates more than 50% viability for both L6 and Hep-2 cells. Cancer cell lines (Hep-2) were more prone to killing by cobalt ferrite nanostructures as compared to normal cell lines, which explains its biocompatibility. This corroborates that such nanostructures can be exploited as drug-delivery vehicles for cancer therapeutics.

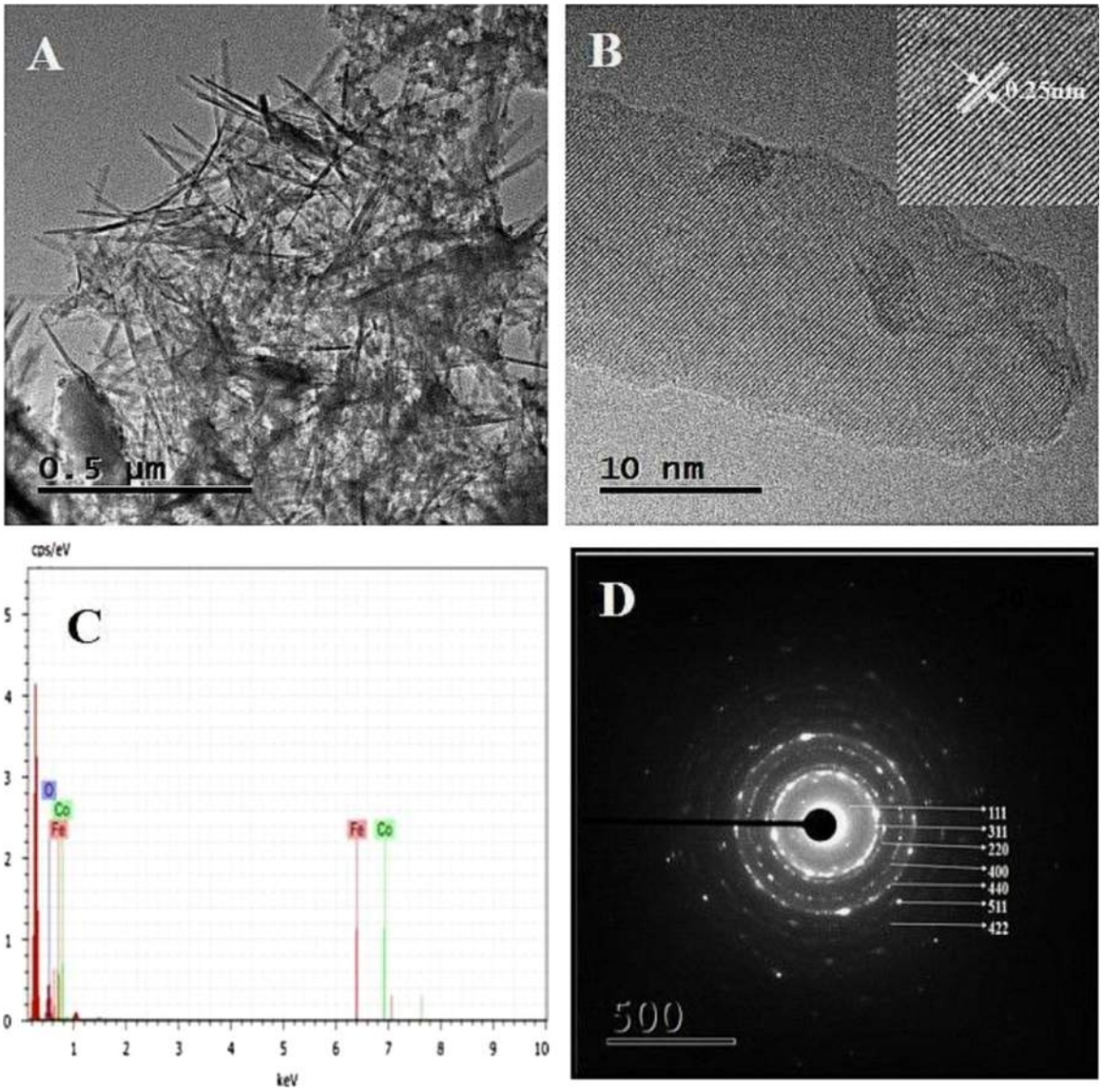


**Fig. 2. A)** TEM micrograph of the $CoFe_2O_4$ nano-needles **B)** HRTEM micrograph of the $CoFe_2O_4$ nano-needles and inset shows IFFT of $CoFe_2O_4$ nano-needles. **C)** Elemental composition of $CoFe_2O_4$ nano-needles. **D)** SAED pattern of $CoFe_2O_4$ nano-needles.

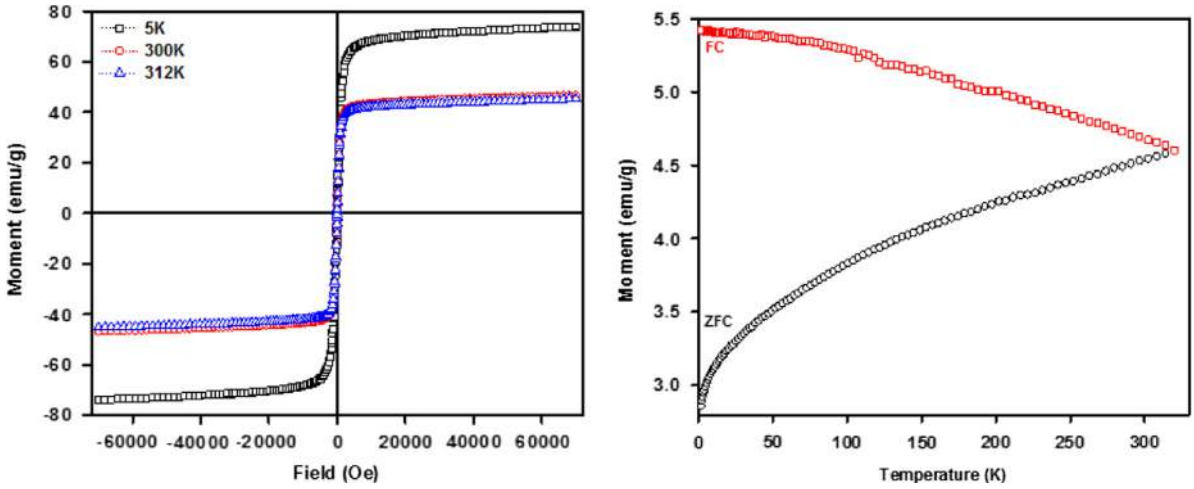


**Fig. 3. A)** Magnetic hysteresis curves of the $CoFe_2O_4$ nano-needles at 5 K, 300 K and 312 K **B)** shows ZFC and FC curves of $CoFe_2O_4$ nano-needles.

**Table 1**
shows the value of magnetic hysteresis curve of $CoFe_2O_4$ nano-needles at 5 K, 300 K and 312 K.

| $CoFe_2O_4$ | Hc (Oe) | Mr (emu/g) | Ms (emu/g) |
|---|---|---|---|
| **5 K** | −145.84 | 7.53 | 74.03 |
| **300 K** | −7.42 | 0.39 | 46.72 |
| **312 K** | −25.38 | 0.24 | 45.39 |

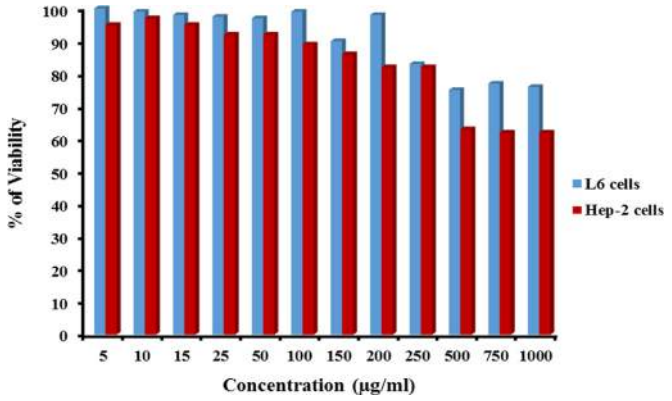


**Fig. 4.** MTT assay of $CoFe_2O_4$ nano-needles on L6 cell lines and Hep-2 cell lines.

## 4. Conclusions

The co-precipitation method exploited for one-pot synthesis of $CoFe_2O_4$ nano-needles has been reported in this communication. The smooth nucleation and regulated growth of needle on one particular plane, which is thermodynamically favorable at high temperatures led to anisotropic nanostructures. The magneto-crystalline anisotropy as well as negligible hysteresis proves its superparamagnetic nature. Such particles exhibit high stability and biocompatibility, which can be used for biomedical applications.

## Acknowledgements

We thank Mr.Alvaro Pascual for HR-TEM analysis and highly acknowledge for the kind financial support given by CONACYT (Project no. 168577).

## Appendix A. Supporting information

Supplementary data associated with this article can be found in the online version at http://dx.doi.org/10.1016/j.matlet.2014.07.154.

## References

[1] Kaushik A, Khan R, Solanki PR, Pandey P, Alam J, Ahmad S. Iron oxide nanoparticles–chitosan composite based glucose biosensor. Biosens Bioelectron 2008;24:676–83.
[2] Sun S, Murray CB, Weller D, Folks L, Moser A. Monodisperse FePt nanoparticles and ferromagnetic FePt nanocrystal superlattices. Science 2000;287:1989–92.
[3] Sugimoto T, Matijevic E. Formation of uniform spherical magnetite particles by crystallization from ferrous hydroxide gels. J Colloid Interface Sci 1980;74:227–43.
[4] Chin AB, Yaacob II. Synthesis and characterization of magnetic iron oxide nanoparticles via w/o microemulsion and Massart's procedure. J Mater Process Technol 2007;191:235–7.
[5] Albornoz C, Jacobo SE. Preparation of a biocompatible magnetic film from an aqueous ferrofluid. J Magn Magn Mater 2006;305:12–5.
[6] Kimata M, Nakagawa D, Hasegawa M. Preparation of monodisperse magnetic particles by hydrolysis of iron alkoxide. Powder Technol 2003;132:112.
[7] Hornbaker DJ, Kahng SJ, Misra S, Smith BW, Johnson AT, Mele EJ. Mapping the one-dimensional electronic states of nanotube peapod structures. Science 2002;295:828–31.
[8] Abedini Khorrami S, Mahmoudzadeh G, Madani SS, Sepehr SS, Manil S, Moradi S, et al. Determination of magnetic properties of nano-size cofe2o4 particles synthesized by combination of sol–gel auto-combustion and ultrasonic irradiation techniques. J Theor Appl Phys 2010;4–2:1–4.
[9] Peddis D, Yaacoub N, Ferretti M, Martinelli A, Piccaluga G, Musinu A, et al. Understanding the formation of ultrafine spinel $CoFe_2O_4$ nanoplatelets and their magnetic properties. J Phys Condens Matter 2012;112:104306.
[10] Wang ZL, Liu Y, Zhang Z. Handbook of nanophase and nanostructure material. New York: Kluwer Academic; 2003.
[11] Zhaoyang L, Guangshun Y, Haitao Z, Jun D, Yongwei Z, Junmin X. Monodisperse silica nanoparticles encapsulating upconversion fluorescent and superparamagnetic nanocrystals. Chem Commun 2008:694–6.
[12] Katalin S, Enik M, Aniko M, Karoly H, Ulla V, Herwig P. Liquid-phase syntheses of cobalt ferrite nanoparticles. J Nanopart Res 2012;14:894.